NOTE

Stereocomplex crystallization and homo-crystallization of star-shaped four-armed stereo diblock poly(lactide)s during precipitation and non-isothermal crystallization

Hideto Tsuji, Nobutsugu Matsumura and Yuki Arakawa

INTRODUCTION

Poly(L-lactide) (PLLA) is a biobased biodegradable polyester that can be used in various applications, such as commodity, industrial, biomedical, pharmaceutical and environmental applications.[1] The stereocomplexed materials from enantiomeric PLLA and poly (D-lactide) (PDLA) have attracted much attention as advanced poly (lactide) (PLA)-based materials because of their superior mechanical performance as well as the hydrolytic/thermal degradation resistance of stereocomplexed PLA materials compared with that of conventional PLA-based materials.[2–4] Stereocomplex (SC)-crystallization in enantiomeric polymer blends containing both linear one-armed PLLA and PDLA (1-L and 1-D, respectively)[2–8] and linear one-armed stereoblock copolymers[2–4,9–12] has been extensively studied. Stereoblock copolymerization is effective at facilitating SC-crystallization because PLLA and PDLA blocks are next to each other. The effects of the star-shaped or branching architecture on SC-crystallization were investigated using blends of both multiarmed PLLA and PDLA,[13] blends of 1-L and multiarmed PDLA and multiarmed PLLA and 1-D[14] and miktoarmed PLLA and PDLA.[15] A star-shaped or branching architecture disturbs the SC-crystallization.

Similar to linear one-armed stereoblock PLA,[11] only SC-crystallites were formed in star-shaped four-armed stereo diblock equimolar PLA (4-LD) polymers.[16] In the present article as well as in previous articles, 'equimolar' means that a polymer contains the same amounts of L- and D-lactyl units. Recently, stereo diblock copolymers of PLA polymers with different arm numbers and high molecular weights were synthesized, and their isothermal and non-isothermal crystallization was investigated.[17] The melting temperature, degree of crystallinity, spherulitic growth rate, crystallite size, long period and crystalline layer thickness of stereo diblock copolymers of PLA polymers decreased with increasing branch number owing to the retarding effect of branching on the crystallization rate and crystallizability. In previous studies,[16,18] we investigated the static isothermal crystallization of star-shaped 4-LD polymers with different molecular weights or different L-lactyl unit contents as well as a star-shaped 4-L polymer from the melt. Only

SC-crystallites were formed in 4-LD in a L-lactyl unit range from 31% to 72%. Both branching and diblock architectures disturbed the SC-crystallization and spherulite growth of equimolar 4-LD polymers, and the effect of the disturbance was larger for branching architectures than for diblock architectures. However, the branching architecture primarily hindered the simultaneous formation of SC- and homo-crystallites of non-equimolar 4-LD polymers.

In the present study, the crystallization of equimolar 4-LD polymers with different molecular weights and four-armed PLLA (4-L) and 4-LD polymers with different L-lactyl unit contents were investigated during precipitation or non-isothermal crystallization.

EXPERIMENTAL SECTION

The preparation of the materials and the methods of measurement and observation utilized in the present study are described in Supplementary Information (Section S1). The molecular characteristics of the polymers used in the present study are summarized in Table 1, and the molecular structure of 4-LD is shown in Figure 1 along with those of 1-armed stereo diblock PLA (1-LD), 4-L/4-armed PDLA (4-D) and 1-L/1-D blend.

RESULTS

Precipitation

Figures 2a and b show the wide-angle X-ray scattering (WAXD) profiles of the precipitated polymers, and Supplementary Figure S1 shows the magnified WAXD profiles of precipitated 4-L11D5 and 4-L4D11. All the precipitated polymers were crystallizable during precipitation. The equimolar 4-LD polymers exhibited only SC-crystalline diffraction peaks at 12, 21 and 24° (Figure 2a), indicating the sole formation of SC-crystallites in the absence of homo-crystallites irrespective of M_n. However, 4-L polymer 4-L16 (100) and non-equimolar 4-L14D2(93) exhibited only α-form homo-crystalline peaks at 12.5, 15, 17, 19 and 22.5°,[16,18] and non-equimolar 4-L11D5(72) and 4-L4D11(31) (Supplementary Figure S1) exhibited only SC-crystalline peaks at 12 and 21°. The WAXD results indicated

Department of Environmental and Life Sciences, Graduate School of Engineering, Toyohashi University of Technology, Aichi, Japan
Correspondence: Professor H Tsuji, Department of Environmental and Life Sciences, Graduate School of Engineering, Toyohashi University of Technology, Tempaku-cho, Toyohashi, Aichi 441-8580, Japan.
E-mail: tsuji@ens.tut.ac.jp

Table 1 Molecular characteristics of 4-L homopolymers and 4-LD copolymers synthesized in the present study[16,18]

Code[a]	Coinitiator	Lactide/coinitiator (mol/mol) or (w/w)	M_n(NMR)[b] (g mol^{-1})	M_n(GPC)[b] (g mol^{-1})	M_w(GPC)/M_n (GPC)[b]	$[\alpha]^{25}_{589}$[c] (deg dm^{-1} g^{-1} cm^{-3})	L-lactyl unit content (%)
4-L4	Pentaerythritol	26.8[d]	4.40×10^3	6.30×10^3	1.10	−153.3	—
4-L5		33.7[d]	5.33×10^3	8.50×10^3	1.14	−178.1	—
4-L8		68.4[d]	8.37×10^3	1.66×10^4	1.28	−173.5	—
4-L11		82.3[d]	1.05×10^4	2.19×10^4	1.12	−163.5	—
4-L14		117.1[d]	1.43×10^4	2.73×10^4	1.07	−172.1	—
4-L16		137.0[d]	1.63×10^4	3.07×10^4	1.12	−175.1	—
4-L5D4	4-L5	50/50[e]	8.51×10^3	1.52×10^4	1.11	−3.6	51.0
4-L8D8	4-L8		1.62×10^4	3.52×10^4	1.08	−3.4	51.0
4-L16D15	4-L16		—[f]	5.45×10^4	1.08	−4.5	51.3
4-L14D2	4-L14	7/93[e]	1.60×10^4	2.90×10^4	1.26	−151.9	93.4
4-L11D5	4-L11	30/70[e]	1.62×10^4	3.12×10^4	1.08	−76.0	71.7
4-L4D11	4-L4	70/30[e]	1.53×10^4	2.64×10^4	1.24	68.1	30.6

Abbreviations: GPC, gel permeation chromatography; NMR, nuclear magnetic resonance; 4-L, 4-armed poly(lactide); 4-LD, 4-armed stereo diblock poly(lactide).
[a]The figure following the letters indicates the M_n value/10^3.
[b]M_n and M_w are the number- and weight-average molecular weights, respectively.
[c]Specific optical rotation measured in a mixed solvent consisting of chloroform/HFIP (vol/vol = 95/5).
[d]In mol/mol.
[e]In w/w.
[f]M_n(NMR) could not be obtained owing to the low fraction of hydroxyl terminal groups, and the molecular weight of the PDLA segments was estimated from the L-lactyl unit content.

that only α-form homo-crystallization and SC-crystallization occurred in the former and latter samples, respectively, during precipitation. Based on the relative peak heights, the broad peaks at approximately 15 and 17° in non-equimolar 4-L11D5(72) and 4-L4D11(31) may be due to the meta phase. For the 4-LD and 4-L polymers with different L-lactyl unit contents, the crystalline species changed from only SC-crystallites to only homo-crystallites with deviation of the L-lactyl unit content from 50%, which is in contrast to that observed for the 1-L/1-D blends.[9] In these blends, the crystalline species changed from only SC-crystallites to both SC- and homo-crystallites and then to only homo-crystallites. The crystallinity (X_c) values of the homo-crystallites (X_c(H)) and SC-crystallites (X_c(S)) of the precipitated polymers estimated from Figures 2a and b are listed in Supplementary Table S1. The X_c(S) values of the equimolar 4-LD polymers (45–56%) increased with increasing M_n, and even an incorporation 7% D-lactyl units in 4-L14D2 resulted in a 16% decrease in X_c(H) compared with that observed for the 4-L homopolymer (4-L16).

Figures 3a and b show the differential scanning calorimetric thermograms of the precipitated polymers for heating. The glass transition, cold crystallization and melting peaks were observed at 35–58 °C, 99–115 °C and 130–213 °C, respectively. The thermal properties obtained from Figures 3a and b are tabulated in Supplementary Table S1. The melting peaks of the SC-crystallites of the equimolar 4-LD polymers were observed at 130–213 °C. 4-L16 (100) exhibited a cold crystallization peak and a melting peak for the homo-crystallites at 107 and 151 °C, respectively. However, 4-L14D2 (93), which contained 7% D-lactyl units, had a lower T_{cc} and T_m for the homo-crystallites (99 and 145 °C, respectively) than those of the optically pure 4-L16. Based on the length of the longer L-lactyl unit block or D-lactyl unit block in 4-L11D5(72) and 4-L4D11(31) being shorter than that in 4-L14D2(93), 4-L11D5(72) and 4-L4D11(31) should exhibit T_m values lower than that of 4-L14D2 with only homo-crystallites if these three polymers only formed homo-crystallites. However, the T_m values of 4-L11D5 and 4-L4D11 (156 and 143 °C, respectively) were higher than and similar to that of 4-L14D2 (145 °C), indicating that these meting peaks correspond to SC-crystallites. The presence of cold crystallization peaks in the DSC thermograms and very low X_c(S) values for 4-L11D5 and 4-L4D11 indicate that, in

addition to the SC-crystallites formed during precipitation, further SC-crystallization occurred during the DSC heating scan.

Non-isothermal crystallization during heating

Figures 3c and d show the DSC thermograms of the melt-quenched samples for heating. All the samples, excluding melt-quenched 4-L11D5(72) and 4-L4D11(31), exhibited cold crystallization, indicating SC- or homo-crystallizability during heating. The thermal properties obtained from Figures 3c and d are summarized in Supplementary Table S1. The similar T_m values of the precipitated and melt-quenched samples strongly suggest that the crystalline species formed during heating of the melt-quenched samples were the same as those formed during precipitation. Therefore, only SC-crystallites were formed in the equimolar 4-LD polymers (4-L5D, 4-L8D8 and 4-L16D15), and only homo-crystallites were formed in 4-L16 and 4-L14D2.

The T_g, T_{cc} and T_m of the SC-crystallites (T_m(S)) values for equimolar 4-LD polymers are plotted in Figure 4 as a function of M_n(NMR) (nuclear magnetic resonance) (T_g and T_{cc}) or M_n(NMR) per one block (T_m(S)) along with those reported for equimolar 1-LD polymers[11] and equimolar 4-L/4-D and 1-L/1-D blends.[13] The linear one-armed 1-L/1-D blends exhibited the highest T_g values except for the T_g of the lowest molecular weight 1-LD polymer. The T_g values decreased with the factors of the branching and diblock architectures, and the T_g values of the 4-LD and 1-LD polymers were lower than those of the 4-L/4-D and 1-L/1-D blends, respectively. The T_g values of the 4-LD and 1-LD polymers were similar to one another and the lowest among the samples. However, the T_{cc} values do not appear to be affected by the branching and diblock architectures. The T_{cc} of the 4-L/4-D blends and 1-LD polymers increased in the low temperature range even though T_{cc} typically decreases with decreasing M_n, as observed for the 1-L/1-D blends. The T_m(S) values of the 1-L/1-D and 4-L/4-D blends as well as the 1-LD and 4-LD polymers were determined by the M_n(NMR) values per one block and not M_n (NMR) or M_n(NMR) per one arm (Supplementary Figure S2). Therefore, the T_m(S) values were determined by the M_n(NMR) values per one block and are not affected by the presence of branching moiety points or turnover points. However, the $-\Delta H_{cc}$ values of the equimolar 4-LD polymers as an index of the maximum crystallinity

a

4-LD

b

4-LD

4-L/4-D

1-LD
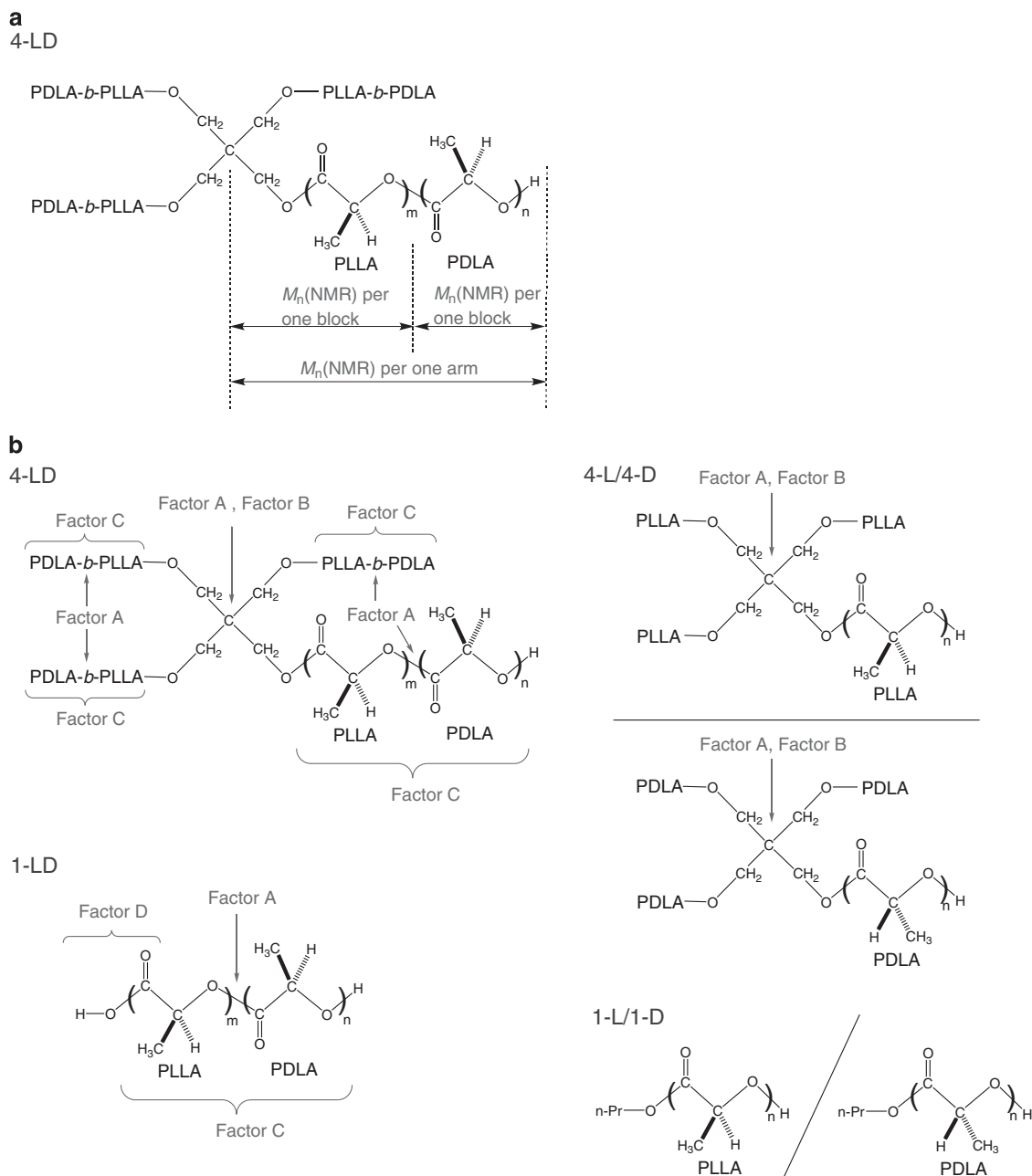
1-L/1-D

Figure 1 Molecular structure of 4-LD, M_n(NMR) per one arm and M_n(NMR) per one block (**a**) and molecular structure of 4-LD, 1-LD, 4-L/4-D and 1-L/1-D blends. Factor A (branching or turnover points), Factor B (intersegmental connection), Factor C (presence of PLLA and PDLA segments in a same molecule) and Factor D (presence of terminal carboxyl group) (**b**). A full color version of this figure is available at the *Polymer Journal* online.

during heating were constant in the 42–45% range, and the $-\Delta H_{cc}$ values of non-equimolar 4-LD polymers were nil. The $-\Delta H_{cc}$ value of 4-L16 (35%) substantially decreased upon incorporation of 7% D-lactyl units (4-L14D2, 7%).

The Flory-Fox and Flory equations were utilized to estimate the T_g and T_m values at infinite molecular weight (T_g^∞ and T_m^∞, respectively) (Section S5 including Supplementary Figure S3). Here, owing to the extraordinary trend stated in the Discussion section, the results for the 1-LD polymers are not compared with those for other samples. The estimated T_g^∞ decreased in the following order: 1-L/1-D blends (60.6 °C) > 4-L/4-D blends (59.1 °C) > 4-LD polymers (53.2 °C) for M_n(NMR) and 1-L/1-D blends (61.3 °C) > 4-L/4-D blends (58.1 °C)

> 4-LD polymers (54.8 °C) for M_n(GPC) (gas permeation chromatography). The evaluated K values or the excess free volume of the terminal groups decreased in the following order: 4-LD polymers (1.2 × 10⁵ K g mol⁻¹) > 4-L/4-D blends (9.9 × 10⁴ K g mol⁻¹) > 1-L/1-D blends (8.9 × 10⁴ K g mol⁻¹) for M_n(NMR) and 4-LD polymers (2.4 × 10⁵ K g mol⁻¹) > 1-L/1-D blends (1.4 × 10⁴ K g mol⁻¹) > 4-L/4-D blends (1.2 × 10⁵ K g mol⁻¹) for M_n(GPC). In addition, the estimated T_m^∞ values decreased in the following order: 1-L/1-D blend (255.3 °C) > 4-L/4-D blends (245.1 °C) > 4-LD polymers (222.9 °C) for M_n(NMR) and 1-L/1-D blend (258.0 °C) > 4-L/4-D blends (240.0 °C) > 4-LD polymers (220.0 °C) for M_n(GPC). These results indicate that the branching and stereo diblock architectures affect the
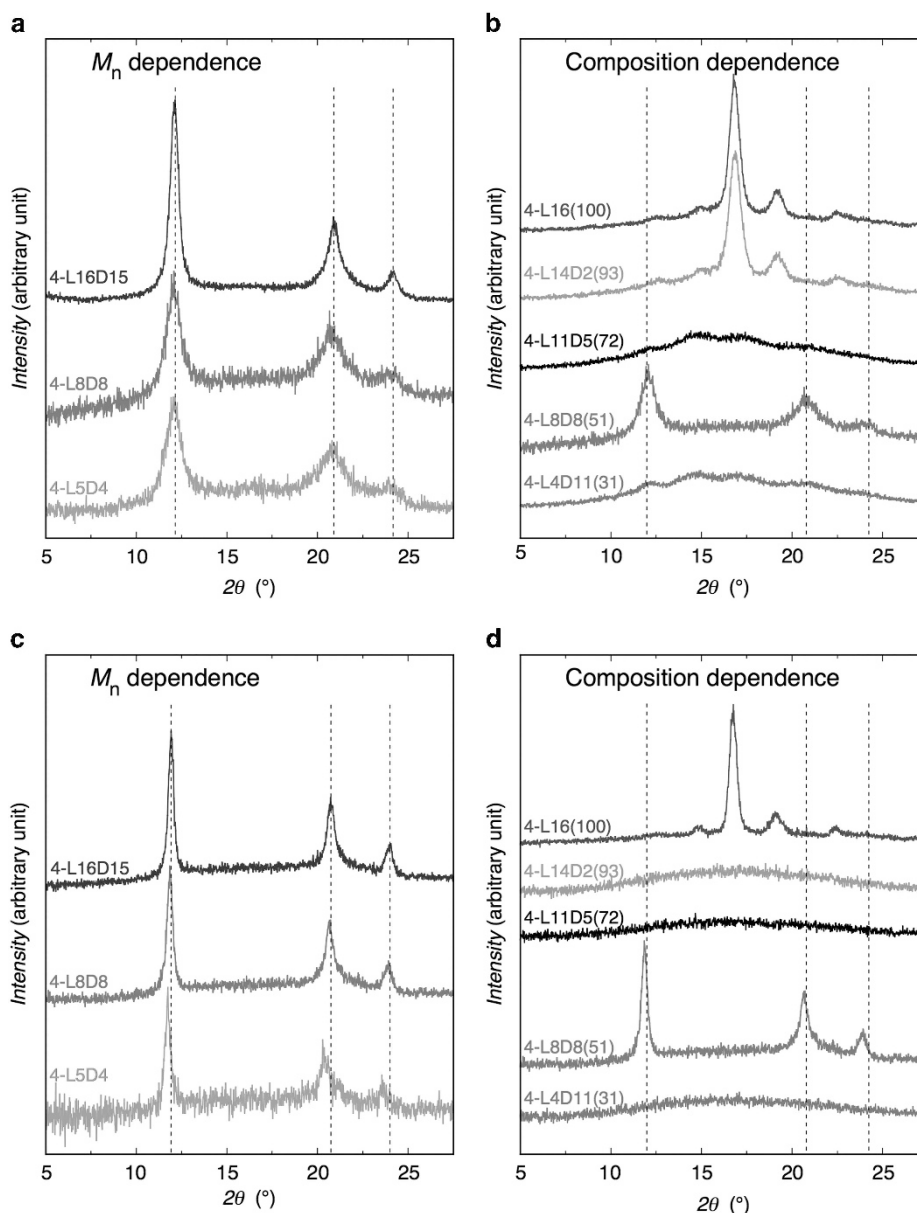
Figure 2 WAXD profiles of precipitated equimolar 4-LD polymers with different M_n values (**a**) and precipitated 4-LD and 4-L polymers with similar M_n values and different L-lactyl unit contents (**b**). WAXD profiles of precipitated equimolar 4-LD polymers with different M_n values (**c**) and 4-LD and 4-L polymers with similar M_n values and different L-lactyl unit contents (**d**) after slow cooling from the melt. The values in the parentheses in panels (**b** and **d**) are the L-lactyl unit contents. A full color version of this figure is available at the *Polymer Journal* online.

chain mobility, excess free volume and crystalline size and disorder at infinite M_n.

Non-isothermal crystallization during cooling

Figures 3e and f show the DSC thermograms of the precipitated samples for slow cooling from the melt. The thermal properties estimated from Figures 3e and f are summarized in Supplementary Table S2. Although equimolar 4-LD polymers and 4-L16 were crystallizable during slow cooling, other polymers were non-crystallizable during slow cooling. In contrast, 4-L14D2 was crystallizable during precipitation and heating as well as isothermal crystallization for 3 h,[18] and 4-L11D5 and 4-L4D11 were crystallizable during precipitation as well as isothermal crystallization for 24 h.[18] As

expected, the sample with a high T_m had a high T_c and onset temperature of crystallization.

Figures 2c and d show the WAXD profiles of the samples after slow cooling from the melt. The $X_c(H)$ and $X_c(S)$ values were evaluated from Figures 2c and d and summarized in Supplementary Table S2. 4-L5D4, 4-L8D8 and 4-L16D15 were crystallized during slow cooling, which is in agreement with the DSC results, and only crystalline diffraction peaks at 12, 21 and 24° that correspond to SC-crystallites were observed for all the equimolar 4-LD polymers. This result indicates the sole formation of SC-crystallites in the equimolar 4-LD polymers without the formation of homo-crystallites irrespective of M_n. However, for 4-L and non-equimolar 4-LD polymers, only 4-L16 (100) was crystallizable during slow cooling, and only α-form homo-crystalline peaks were observed at 15, 17, 19 and 22.5°.
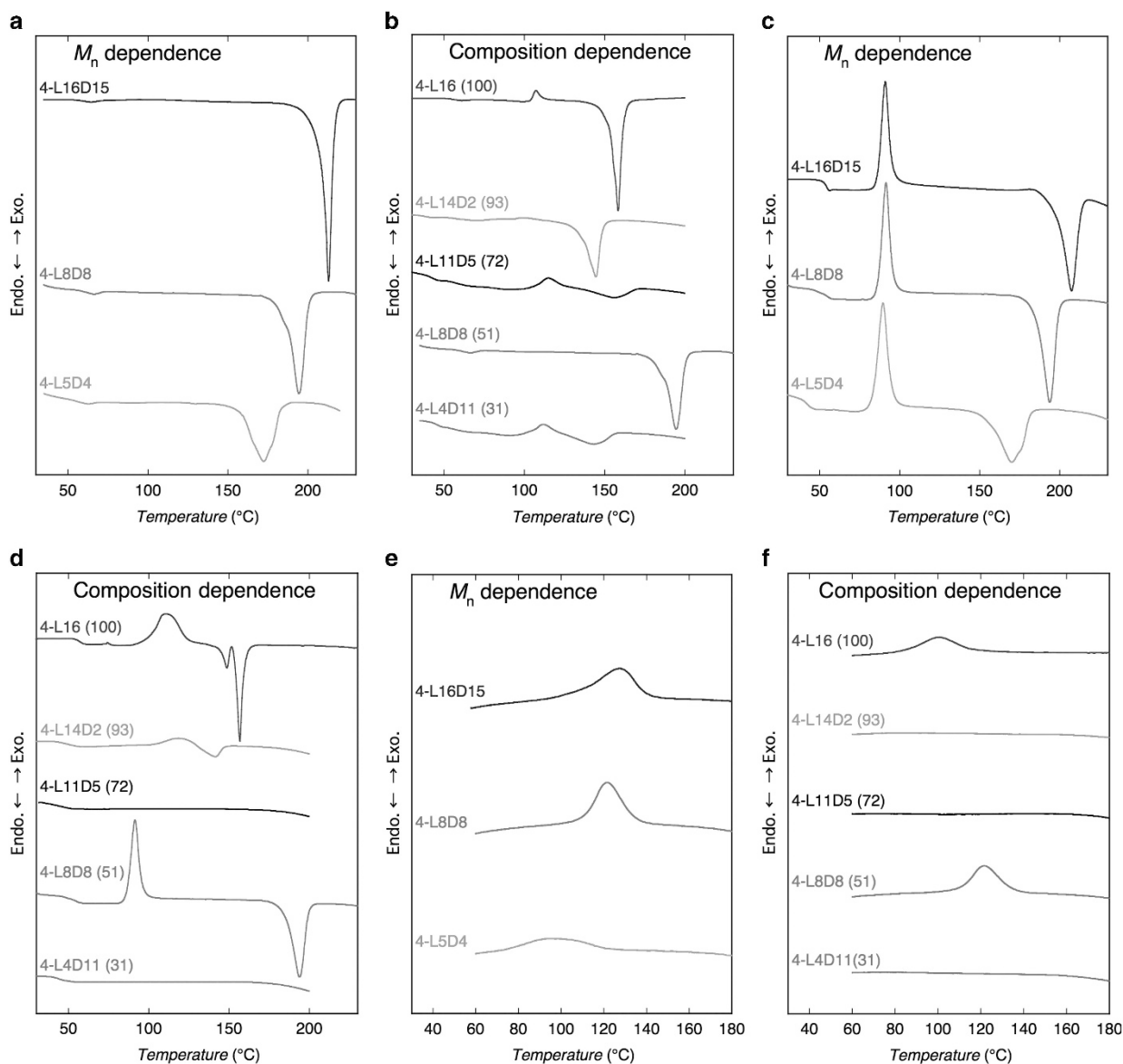
Figure 3 DSC thermograms of precipitated (**a**, **b**) and melt-quenched (**c**, **d**) equimolar 4-LD polymers with different M_n values (**a**, **c**) and precipitated 4-LD and 4-L polymers with similar M_n values and different L-lactyl unit contents (**b**, **d**) for heating. DSC thermograms of precipitated equimolar 4-LD polymers with different M_n values (**e**) and 4-LD and 4-L polymers with similar M_n values and different L-lactyl unit contents (**f**) for slow cooling from the melt. The values in the parentheses in panels (**b**, **d** and **f**) are the L-lactyl unit contents. A full color version of this figure is available at the *Polymer Journal* online.

Avrami analysis

The overall crystallization kinetics that was traced by DSC was analyzed according to the Avrami theory (Supplementary Information (Section S6 including Supplementary Figures S4–S7)). The values of the Avrami exponent (n), crystallization rate constant (k) and experimental and calculated crystallization half times ($t_c(1/2)$ (exp) and $t_c(1/2)$(cal), respectively) are summarized in Supplementary Table S3. For heating, assuming thermal nucleation, the n values of equimolar 4-LD polymers (that is, approximately 5) indicate a solid sheaf growth morphology, and n values of approximately 3 for 4-L16 and 4-L14D2 indicate a circular growth morphology.[19] These results strongly suggest that the growth morphology was dependent on the crystalline species (SC- or homo-crystallites). For slow cooling, the n values of equimolar 4-LD polymers increased from 2.15 for 4-L5D4 to 3.49 for 4-L16D15 with an increase in M_n, indicating a fibrillar or

circular growth morphology assuming thermal nucleation, and an n value of 4-L16 (2.68) reflects the circular growth morphology. The n values of equimolar 4-L8D8 (3.03) and optically pure 4-L16 (2.68) possessed similar M_n values, indicating that the type of crystalline species or block copolymerization does not affect the growth morphology.

DISCUSSION

As the M_n of branching polymers or stereo diblock copolymers (4-LD and 1-LD polymers, 4-L/4-D blends) decreased, the effects of branching or turnover points where the change in the chain direction or configuration occurs become higher owing to increased branching or turnover points per unit mass at a lower molecular weight. These branching or turnover points should disturb close packing or interactions between the segments and increase the free volume
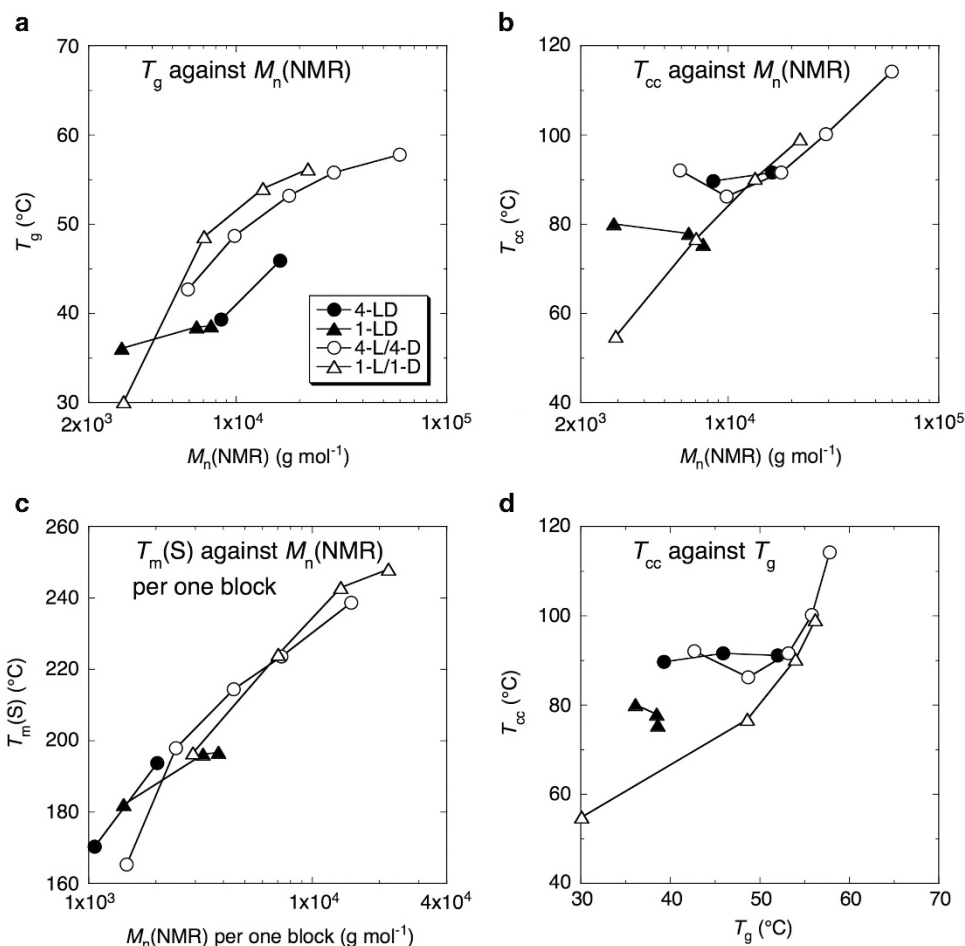
Figure 4 T_g (**a**) and T_{cc} (**b**) as a function of M_n(NMR), T_m(S) as a function of M_n(NMR) per one block (**c**) and T_{cc} as a function of T_g (**d**) for equimolar 4-LD and 1-LD polymers as well as the 4-L/4-D and 1-L/1-D blends. T_g, T_{cc} and T_m(S) values for equimolar 1-LD and 4-L/4-D as well as the 1-L/1-D blends are those reported in Tsuji *et al.*[11] and Sakamoto and Tsuji[13], respectively.

(Factor A). This factor will increase the segmental mobility, resulting in a decrease in T_g and T_{cc} or acceleration of cold crystallization. The intersegmental connection (4-LD polymers, 4-L/4-D blends) owing to branching moieties is expected to lower the segmental mobility and disturb segmental diffusion to the crystalline growth sites (Factor B), resulting in an increase in T_g and T_{cc} or delayed cold crystallization. As reported for two-armed PLLA/PDLA blends and PLLA-*b*-PDLA,[20] the presence of PLLA and PDLA segments in the same molecule (Factor C) (for example, 4-LD and 1-LD polymers) can disturb SC-crystallization compared with that of homopolymer blends (4-L/4-D blends and 1-L/1-D blends, respectively) even though the detailed mechanism for this factor has not been clarified. In addition, it is important to note that the terminals of 4-LD and 4-L/4-D[13] are hydroxyl groups, and the terminals of 1-L/1-D are hydroxyl and *n*-propyl ester groups.[13] However, the terminals of 1-LD are hydroxyl and carboxyl groups.[11] The presence of terminal carboxyl groups in 1-LD, which can form strong hydrogen bonds with ester groups inside the chain, terminal hydroxyl groups or terminal carboxyl groups, will increase the interchain interaction (Factor D), which will increase the seeming molecular weight and result in decreased segmental mobility (that is, high T_g) and disturbed segmental diffusion to the crystalline growth site (that is, high T_{cc}), especially at a low M_n value. The extraordinary trends in T_g and T_{cc} for the lowest molecular weight of

1-LD observed in Figure 4 and Supplementary Figure S3 are due to Factor D. Factors A–D are illustrated in Figure 1b.

The lower T_g values of the 4-LD and 1-LD polymers compared with those of the 4-L/4-D and 1-L/1-D blends, respectively (Figure 4a), were due to Factor A regarding the turnover points of the configurational change. However, despite the addition of Factor B to 1-LD, the unaltered T_g values of 4-LD compared with those of the 1-LD polymers indicates that Factor A for the branching moieties, Factor B and Factor D were counterbalanced. For further discussion, T_{cc} is replotted in Figure 4d as a function of T_g to exclude the effects of segmental mobility on T_{cc}. Based on the T_{cc} values shown in this plot, cold crystallization was disturbed in the following order: 4-LD polymers $\approx$ 4-L/4-D blends > 1-LD polymers > 1-L/1-D blends. This result indicates that the disturbed cold crystallization was observed for the 4-L/4-D blends as well as the 4-LD and 1-LD polymers compared with the 1-L/1-D blends. When the effects of segmental mobility are excluded, the higher T_{cc} values of the 4-L/4-D blends and 4-LD polymers compared with those of the 1-L/1-D blends may be due to disturbed segmental diffusion (Factor B). The high T_{cc} values of the 1-LD polymers compared with those of the 1-L/1-D blends were due to disturbed segmental diffusion (Factor D). It is interesting to note that the similar T_{cc} values for the 4-L/4-D blends and 4-LD polymers indicate that further addition of Factor C does not disturb the cold crystallization.

SC-crystallization of 4-L11D5(72) and 4-L4D11(31), which required isothermal crystallization for 24 h from the melt,[18] could be readily attained by precipitation in a short time period, such as several seconds. The crystalline species changed directly from only SC-crystallites to amorphous and then to only homo-crystallites (during non-isothermal crystallization) or from only SC-crystallites to only homo-crystallites (during precipitation) with deviation of L-lactyl unit content from 50%. This result is in contrast to the result for 1-LD, where these crystalline species changed from only SC-crystallites to both SC- and homo-crystallites and then to only homo-crystallites.[9] A comparison of the results for the 4-LD and 1-LD polymers strongly suggests that the branching architecture rather than the diblock architecture disturbed the simultaneous formation of SC- and homo-crystallites.

CONCLUSIONS

All the equimolar 4-LD polymers formed only SC-crystallites during precipitation, heating from ambient temperature or slow cooling from the melt irrespective of M_n. During precipitation, the 4-L and non-equimolar 4-LD polymers with L-lactyl unit contents of 100% and 93% formed only α-form homo-crystallites, and non-equimolar 4-LD polymers with L-lactyl unit contents of 72% and 31% formed only SC-crystallites. During heating, the 4-L and non-equimolar 4-LD polymers with L-lactyl unit contents of 100% and 93% formed only homo-crystallites, and the other non-equimolar 4-LD polymers were non-crystallizable. During slow cooling, the 4-L homopolymer formed only α-form homo-crystallites, and the other non-equimolar 4-LD polymers were non-crystallizable. With the deviation of the L-lactyl unit content from 50%, the crystalline species of the 4-LD polymers changed from only SC-crystallites to an amorphous form and then to only homo-crystallites (during non-isothermal crystallization) or from only SC-crystallites to only homo-crystallites (during precipitation). The branching architecture rather than the stereo diblock architecture disturbed the simultaneous formation of SC-crystallites and homo-crystallites. The crystallite growth morphology during heating depended on the crystalline species, and the crystallite growth morphology during slow cooling was not altered by the crystalline species or block copolymerization. Factor A decreased T_g, and the higher T_{cc} values of the 4-L/4-D blends and 4-LD polymers compared with those of the 1-L/1-D blends were due to disturbed segmental diffusion (Factor B). In addition, the high T_{cc} values of the 1-LD polymers compared with those of the 1-L/1-D blends were due to disturbed segmental diffusion (Factor D).

CONFLICT OF INTEREST

The authors declare no conflict of interest.

1   Slager, J. & Domb, A. J. Biopolymer stereocomplexes. *Adv. Drug Deliv. Rev.* **55**, 549–583 (2003).
2   Tsuji, H. Poly(lactide) stereocomplexes: formation, structure, properties, degradation, and applications. *Macromol. Biosci.* **5**, 569–597 (2005).
3   Tsuji, H. Poly(lactic acid) stereocomplexes: a progress of decade. *Adv. Drug Del. Rev.* doi:10.1016/j.addr.2016.04.017 (in press).
4   Tsuji, H., Ikada, Y., Hyon, S. H., Kimura, Y. & Kitao, T. Stereocomplex formation between enantiomeric poly(lactic acid). VIII. Complex fibers spun from mixed solution of poly(D-lactic acid) and poly(L-lactic acid). *J. Appl. Polym. Sci.* **51**, 337–344 (1994).
5   Serizawa, T., Yamashita, H, Fujiwara, T., Kimura, Y. & Akashi, M. Stepwise assembly of enantiomeric poly(lactide)s on surfaces. *Macromolecules* **34**, 1996–2001 (2001)
6   Takasaki, M., Ito, H. & Kikutani, T. Development of stereocomplex crystal of polylactide in high-speed melt spinning and subsequent drawing and annealing processes. *J. Macromol. Sci. Phys.* **42B**(3-4 SPEC.), 403–420 (2003).
7   Fujita, M., Sawayanagi, T., Abe, H., Tanaka, T., Iwata, T., Ito, K., Fujisawa, T. & Maeda, M. Stereocomplex formation through reorganization of poly(L-lactic acid) and poly(D-lactic acid) crystals. *Macromolecules* **41**, 2852–2858 (2008).
8   Ishii, D., Ying, T. H., Mahara, A., Murakami, S., Yamaoka, T., Lee, W. & Iwata, T. In vivo tissue response and degradation behavior of PLLA and stereocomplexed PLA nanofibers. *Biomacromolecules* **10**, 237–242 (2009).
9   Li, L., Zhong, Z., De Jeu, W. H., Dijkstra, P. J. & Feijen, J. Crystal structure and morphology of poly(L-lactide-b-D-lactide) diblock copolymers. *Macromolecules* **37**, 8641–8646 (2004).
10 Sugai, N., Yamamoto, T. & Tezuka, Y. Synthesis of orientationally isomeric cyclic stereoblock polylactides with head-to-head and head-to-tail linkages of the enantiomeric segments. *ACS Macro Lett.* **1**, 902–906 (2012).
11 Tsuji, H., Wada, T., Sakamoto, Y. & Sugiura, Y. Stereocomplex crystallization and spherulite growth behavior of poly(L-lactide)-b-poly(D-lactide) stereodiblock copolymers. *Polymer* **51**, 4937–4947 (2010).
12 Masutani, K., Lee, C. W. & Kimura, Y. Synthesis and properties of stereo di- and tri-block polylactides of different block compositions by terminal diels-alder coupling of poly-L-lactide and poly-D-lactide prepolymers. *Polym. J.* **45**, 427–435 (2013).
13 Sakamoto, Y. & Tsuji, H. Stereocomplex crystallization behavior and physical properties of linear 1-arm, 2-arm, and branched 4-arm poly(L-lactide)/poly(D-lactide) blends: effects of chain directional change and branching. *Macromol. Chem. Phys.* **214**, 776–786 (2013).
14 Shao, J., Sun, J., Bian, X., Cui, Y., Li, G. & Xuesi, C. Investigation of poly(lactide) stereocomplexes: 3-armed poly(L-lactide) blended with linear and 3-armed enantiomers. *J. Phys. Chem. B* **116**, 9983–9991 (2012).
15 Isono, T., Kondo, Y., Otsuka, I., Nishiyama, Y., Borsali, R., Kakuchi, T. & Satoh, T. Synthesis and stereocomplex formation of star-shaped stereoblock polylactides consisting of poly(L-lactide) and poly(D-lactide) arms. *Macromolecules* **46**, 8509–8518 (2013).
16 Tsuji, H. & Matsumura, N. Stereocomplex crystallization of star-shaped four-armed stereo diblock poly(lactide)s with different molecular weights: isothermal crystallization from the melt. *Macromol. Chem. Phys.* **217**, 1547–1557 (2006).
17 Han, L., Shan, G., Bao, Y. & Pan, P. Exclusive stereocomplex crystallization of linear and multiarm star-shaped high-molecular-weight stereo diblock poly(lactic acid)s. *J. Phys. Chem. B* **119**, 14270–14279 (2015).
18 Tsuji, H., Matsumura, N. & Arakawa, Y. Stereocomplex crystallization and homocrystallization of star-shaped four-armed stereo diblock poly(lactide)s with different L-lactyl unit contents: isothermal crystallization from the melt. *J. Phys. Chem. B* **120**, 1183–1193 (2016).
19 Gedde U. W. in *Polymer Physics* Ch. 8, 170–98 (Chapman & Hall, London, UK, 1995).
20 Tsuji, H., Tamai, K., Kimura, T., Kubota, A., Tahahashi, A., Kuzuya, A. & Ohya, Y. Stereocomplex- and homo-crystallization of blends from 2-armed poly(L-lactide) and poly(D-lactide) with identical and opposite chain directional architectures and of 2-armed stereo diblock poly(lactide). *Polymer* **96**, 167–181 (2016).

Supplementary Information accompanies the paper on Polymer Journal website (http://www.nature.com/pj)